Classical semimicroscopic model applied to doubly even titanium isotopes

S. M. Abecasis and J. M. Carcione
Laboratorio de Radiaciones, Departamento de Física, Facultad de Ciencias Exactas y Naturales, Universidad de Buenos Aires, Núñez, 1428 Buenos Aires, Argentina
(Received 26 September 1978)

The low-lying positive-parity states of doubly even titanium isotopes are analyzed with the classical semimicroscopic model which involves the coupling of a two-proton cluster to the corresponding vibrational cores. The calculated energy-level sequence and electromagnetic properties compare favorably with experiment although no attempt to the best fit to individual properties was pursued. Comparison with calculated values with other models is also performed.

[NUCLEAR STRUCTURE ^{44}Ti, ^{46}Ti, ^{48}Ti, and ^{52}Ti; calculated levels, J, π, $B(E2)$, $B(M1)$, q, μ, δ, τ, b. Classical semimicroscopic model.]

I. INTRODUCTION

The doubly even titanium isotopes are of particular interest from the theoretical point of view since they exhibit features intermediate between harmonic vibrations and rotations. This behavior is borne out by the level spectra, by enhanced quadrupole electric transitions and large static quadrupole moments for the first excited states. A considerable amount of theoretical work has been devoted to them with different models: phenomenological approaches, shell-model calculation, and microscopic descriptions. However, complete calculations have not been reported as yet.

The success obtained with the classical semimicroscopic model[1] when applied to some nuclei of the $1f$-$2p$ shell[2] has encouraged us to explore the possibilities of its applications to even-mass titanium isotopes which are expected to be adequately described by this model. In the classical semimicroscopic model (SMM) these nuclei can be analyzed in terms of the coupling of a two-proton cluster to the corresponding vibrational cores.

In the present investigation, both a detailed description and comparison of the properties of the low-lying states—energy-level sequence, electromagnetic properties, and lifetimes—with experiment is performed for ^{44}Ti, ^{46}Ti, ^{48}Ti, and ^{52}Ti nuclei. The ^{42}Ti and ^{50}Ti isotopes were excluded from the calculations since their possible cores (the doubly even calcium isotopes) cannot provide a quadrupole vibrational field.

We devote Sec. II to the description of the formalism used, listing only the main formulas needed in the calculations. In Sec. III we give some details of the numerical calculations together with comparisons with other models. Finally, some general conclusions are presented in Sec. IV.

II. FORMALISM

Since a detailed derivation of the formulation of the classical SMM is given elsewhere[1] only some formulas needed to settle ideas on this work are presented here.

Our starting Hamiltonian has the usual form[1]:

$$H = H_{\text{coll}} + H_{\text{sp}} + H_{\text{int}} + H_{\text{res}}, \tag{1}$$

where the Hamiltonians are, respectively, associated with (i) the harmonic quadrupole vibrations of the even core, (ii) the motion of the extracore nucleons in an effective spherical potential, (iii) the interaction of the cluster with the vibrating core in which the interaction strength k is considered to be a fixed parameter, and (iv) the residual two-body interaction within the cluster which is considered to be a pairing interaction with strength G.

Our base vectors are

$$|(j_1 j_2)J, NR; IM\rangle = (|JM_J\rangle \otimes |NRM_R\rangle)_{IM}, \tag{2}$$

where $j_i \equiv n_i l_i j_i$ with n, j and l being the principal, orbital and angular momentum quantum numbers of each particle; $|JM_J\rangle$ is the state vectors of the two-proton cluster with J representing the total angular momentum; $|NRM_R\rangle$ is the state vectors of the vibrating core, with N phonons coupled to angular momentum R; and I and M are the total angular momentum quantum numbers of the even nucleus.

The total Hamiltonian (1) is diagonalized in the

base (2) in which the Hamiltonians $H_{coll}+H_{sp}$ are diagonal.

The eigenstates of the model Hamiltonian are

$$|E;{}^{\kappa}IM\rangle = \sum_{JNR} \eta^{I,E}_{JNR}|(j_1j_2)J, NR; IM\rangle , \quad (3)$$

where the amplitudes $\eta^{I,E}_{JNR}$ are obtained by diagonalizing the energy matrices, and the superindex κ distinguishes between states of the same angular momentum I in order of increasing energy.

The electric quadrupole and magnetic dipole operators are a sum of a particle contribution and a collective one. Their reduced matrix elements are expressed in the form

$$\langle I_f \|E2\| I_i\rangle = Ae^{\text{eff}} + Be^{\text{eff}}_{\text{vib}} , \quad (4)$$

$$\langle I_f \|M1\| I_i\rangle = Cg_R + Dg_l + Eg^{\text{eff}}_s . \quad (5)$$

The following notation is used; e^{eff} is the effective proton charge; $e^{\text{eff}}_{\text{vib}} = Ze\beta\sqrt{5}$ is the effective vibrator charge where β is the quadrupole deformation of the core with Z protons, and e is the bare proton charge; g_R, g_l and g^{eff}_s are the gyromagnetic ratios of the core, orbital and spin parts, respectively; the quantities A, B, C, D and E are calculated by means of the state vectors (3).

The mixing ratios δ, the lifetimes τ, and the branching ratios b are calculated with the usual formulas.[3]

III. RESULTS AND DISCUSSION

In this section we give some details of the calculations, together with a comparison with other models. The calculations were performed with a unique set of single-particle energies.[4] Therefore we are neglecting the A dependence in the level positions, and the "fine structure" superimposed on it.[5]

The parameters β and the phonon energies $\hbar\omega$ were taken, respectively, as the quadrupole deformation and the energy of the $^12+$ states of the corresponding vibrators.[6] However, for the particular cases of ^{44}Ti and ^{46}Ti—which exhibit a $^20+$ state at an energy too low in comparison with that theoretically predicted—the experimental values of the states belonging to the two phonon multiplets were considered. The two-proton states appearing in Eq. (2) are taken as being coupled up to three phonons.

For the pairing strength constant G, we took the values commonly quoted in the literature for this mass region,[7] although a small variation of it and in turn of β was also permitted in order to obtain a better fitting with the experimental level sequence. As concerns the cluster-field interaction strength k, it was kept constant at a fixed value since it is not seriously affected by the particle quantum numbers.[5]

In Table I are listed the adopted values for the adjustable parameters involved in the present calculations for each titanium isotope.

With the set of parameters chosen for each titanium isotope, the first four levels of each spin up to the highest observed one were calculated. Finally, the state vectors of Eq. (3) were used to compute electromagnetic properties, branching and mixing ratios, and lifetimes, all at once in only one program. The calculations were performed with eight combinations of effective charges and gyromagnetic ratios[3]; finally—after comparison with experiment—we adopted the following set of parameters:

Set I: $e^{\text{eff}} = 1.33\ e$ (Ref. 8), $e^{\text{eff}}_{\text{vib}} = Ze\beta/\sqrt{5}$;

Set 1: $g_R = 0$, $g^{\text{eff}}_s = g^{\text{free}}_s = 5.59$.

In the following sections the results for ^{44,46,48,52}Ti isotopes are presented and compared with other models.

A. The ^{44}Ti nucleus

In Table II the main components (amplitudes larger than 4%) of the state vectors of some low-lying positive-parity states for the four titanium isotopes under consideration are listed to make their comparison easier (see Sec. IV).

The resulting energy sequence of positive-parity states of ^{44}Ti are compared in Fig. 1(B) with the experimental data [Fig. 1(A)] (Ref. 8), and with the predictions of other models[9,11,12] [Figs. 1(C)-1(G)]. Khadkikar and Banerjee[9] have calculated the energy levels of ^{44}Ti using the projected Hartree-Fock method [Fig. 1(C)] and the stretch scheme of Danos and Gillet[10] [Fig. 1(D)], in which a truncated configuration space is involved. Later on, Bhatt and McGrory[11] have carried out "exact" shell-model calculations with the same interaction as that used in Ref. 9 [Fig. 1(E)], and these authors repeated their calculations using the Kuo and Brown interaction and experimental single-par-

TABLE I. Values of the adjustable parameters G, β, and $\hbar\omega$ used in the present calculations.

Nuclide	G (MeV)	β	$\hbar\omega$ (MeV)
^{44}Ti	0.6	0.18	1.60
^{46}Ti	0.7	0.21	1.30
^{48}Ti	0.7	0.21	1.53
^{52}Ti	0.7	0.18	1.50

TABLE II. Components $\times 10^3$ of some low-lying positive-parity states for ^{44,46,48,52}Ti calculated with the present model. Each state is indicated by its ordering number and spin. The base vectors are defined in the text.

	^{44}Ti	^{46}Ti	^{48}Ti	^{52}Ti		^{44}Ti	^{46}Ti	^{48}Ti	^{52}Ti
^{1}0					^{1}2				
$\|(f_{7/2},f_{7/2})0,00\rangle$	690	599	669	742	$\|(f_{7/2},f_{7/2})0,12\rangle$	658	594	620	687
$\|(f_{7/2},f_{7/2})2,12\rangle$	−340	−336	−336	−316	$\|(p_{3/2},p_{3/2})0,12\rangle$	274	287	293	300
$\|(f_{7/2},f_{7/2})0,20\rangle$	321	350	262	222	$\|(f_{7/2},f_{7/2})2,00\rangle$	−263	−192	−215	−221
$\|(f_{7/2},p_{3/2})2,12\rangle$	314	343	338	301	$\|(f_{7/2},f_{7/2})2,24\rangle$	−228	−229	−229	−226
$\|(p_{3/2},p_{3/2})0,00\rangle$	287	285	311	319	$\|(f_{7/2},p_{3/2})2,00\rangle$	209	194	206	190
					$\|(f_{7/2},p_{3/2})2,24\rangle$	204	242	234	217
^{1}4					^{2}0				
$\|(f_{7/2},f_{7/2})0,22\rangle$	532	581	572	634	$\|(f_{7/2},f_{7/2})0,20\rangle$	−717	623	−599	−668
$\|(f_{7/2},f_{7/2})2,12\rangle$	−351	−295	−309	−316	$\|(f_{7/2},f_{7/2})0,00\rangle$	501	572	525	442
$\|(f_{7/2},p_{3/2})2,12\rangle$	265	277	283	264	$\|(p_{3/2},p_{3/2})0,20\rangle$	−262	−274	−286	−294
$\|(p_{3/2},p_{3/2})0,24\rangle$	220	283	279	285	$\|(f_{7/2},f_{7/2})2,32\rangle$	246	249	252	256
$\|(f_{7/2},f_{7/2})6,12\rangle$	−216	−150	−165	−146	$\|(f_{7/2},p_{3/2})2,32\rangle$	−220	−243	−261	−248
$\|(f_{7/2},f_{7/2})4,00\rangle$	299	175	207	208					
^{2}2					^{1}6				
$\|(f_{7/2},f_{7/2})0,22\rangle$	599	621	621	676	$\|(f_{7/2},f_{7/2})6,00\rangle$	603	380	469	546
$\|(f_{7/2},f_{7/2})2,12\rangle$	−432	−338	−357	−347	$\|(f_{7/2},f_{7/2})6,12\rangle$	−342	−260	−286	−309
$\|(p_{3/2},p_{3/2})0,20\rangle$	224	277	277	287	$\|(f_{7/2},f_{7/2})4,12\rangle$	−335	−355	−362	−359
$\|(f_{7/2},f_{7/2})4,24\rangle$	221	196	199	179	$\|(f_{7/2},p_{3/2})4,12\rangle$	314	328	337	316
$\|(f_{7/2},f_{7/2})0,12\rangle$	193	271	260	220	$\|(f_{7/2},f_{7/2})6,20\rangle$	275	242	205	193
$\|(f_{7/2},p_{3/2})2,12\rangle$	173	182	194	200	$\|(f_{7/2},f_{7/2})2,24\rangle$	183	286	262	242
					$\|(f_{7/2},f_{7/2})0,36\rangle$	−102	−269	−225	−218
					$\|(f_{7/2},p_{3/2})2,24\rangle$	−126	−238	−213	−185

ticle energies [Fig. 1(F)]. A similar calculation was performed by Vignon *et al.*[12] using the modified surface δ interaction (MSDI)[13] [Fig. 1(G)]. Inspection of Figs. 1(F) and 1(G) indicate that conventional shell-model calculations yield similar results, rather independently of the interaction involved, and they are in better agreement with experiment than those obtained with the approximation used in Ref. 9. The noticeable similarity among these calculations is the strong deviation from the $I(I+1)$ spacing of the rigid rotator. Conversely, the main differences are connected with the "compression" of the ^{1}8+ level and the clear separation between the ground state "band" and the "higher" bands which are the characteristic features of Khadkikar and Banerjee calculations. However, none of these calculations can reproduce either the level density or the position of the ^{2}0+ level. Both facts are described by the present model, even when the ^{2}0+ state is predicted in inverse order with respect to the ^{1}4+ one.

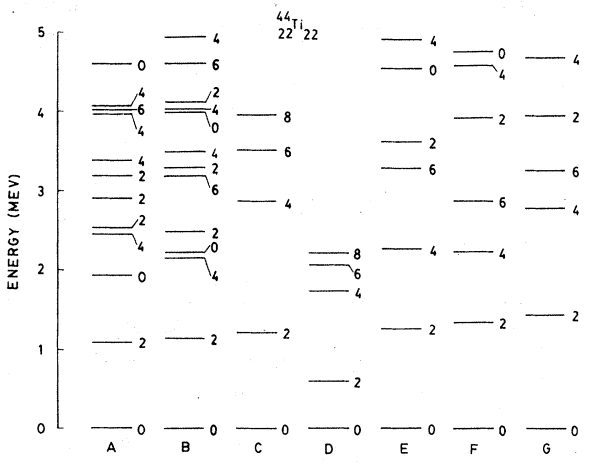

FIG. 1. Experimental and theoretical low-lying positive-parity level sequence for ^{44}Ti. A: Experiment (Ref. 8). B: Present model. C and D: Ref. 9. E and F: Ref. 11. G: Ref. 12.

Insofar as the electromagnetic properties are concerned, their values calculated with the present model are compared in Table III with experimental values. Also listed, for the sake of completeness, are the values for the static quadrupole moment of the ^{1}2+ state and $E2$ transition rates calculated within the framework of the strong coupling rotational model,[14] shell model,[14-17] as well as the Hartree-Fock-Bogoliubov formalism.[18] No experimental data on the quadrupole moment of the ^{1}2+ states are available, but we include other theoretical results to show comparative trends between our model and the others. The rather large negative quadrupole moments of the ^{1}2, ^{1}4 and ^{1}6 states and the enhanced $E2$ transition between them favor the assumption of a

TABLE III. Experimental and theoretical energy values of some low-lying positive-parity states for ^{44}Ti and those corresponding to the electromagnetic properties. The values calculated with other models are indicated by OM; the set of values for the effective proton and vibrator charges, and gyromagnetic ratios are indicated in the text.

		E (keV)		Q (eb) Theory		μ (μ_N) Theory	τ (ps)	
$^{\kappa}I$		Exp.[a]	Theory	I	OM	1	Exp.[b]	Theory $I+1$
$^{1}2$		1082.9 ± 0.1	1133.8	−0.141	−0.127[c] 0.179[d] 0.071[d]	0.736	4.50 ± 1.1	2.57
$^{2}0$		1904.2 ± 0.8	2250.5				>0.7	10.12
$^{1}4$		2454.1 ± 0.3	2228.1	−0.165		2.880	0.60 ± 0.1	2.20
$^{2}2$		2530.6 ± 0.2	2454.9	0.129		0.886	1.40 ± 0.2	0.99
$^{3}2$		2886.2 ± 0.6	3257.0	0.152		3.230	0.50 ± 0.1	0.007
$^{4}2$		3175.8 ± 0.8	4165.4	−0.060		2.961	>3.0	0.003
$^{2}4$		3365 ± 5	3465.3	−0.141		4.059	0.60 ± 0.2	0.01
$^{3}4$		3980 ± 5	4026.0	−0.018		3.857	0.50 ± 0.2	0.12
($^{1}6$)		4015 ± 5	3172.7	−0.285		8.152	0.56 ± 0.08	7.79
		4060 ± 5	4925.6	0.071		5.600	$2.10^{+1.9}_{-0.7}$	0.03

		$B(E2)$ (W.u.)			$B(M1)$ (W.u.)		δ		b (%)	
			Theory			Theory		Theory		Theory
$^{\kappa}I_i$	$^{\kappa}I_f$	Exp.[e]	I	OM	Exp.	1	Exp.	$I+1$	Exp.[b]	$I+1$
$^{1}2$	$^{1}0$	13 ± 4	18.34	14.30[c] 13.11[e] 9.61[d] 11.51[d] 6.28[g] 12.57[h] 12.68[i]					100	100
$^{2}0$	$^{1}2$	<330	5.03						100	100
$^{1}4$	$^{1}2$	30 ± 6	25.54	18.00[e] 9.21[g] 17.55[g] 16.69[i]					100	100
$^{2}2$	$^{2}0$	24 ± 6	0.02						3.7 ± 0.5	0.81×10^{-5}
$^{2}2$	$^{1}2$	7 ± 1.3	20.43	0.009[d] 15.57[d]		0.10×10^{-3}	−7.5[j]	−11.23	71 ± 5	92.57
$^{2}2$	$^{1}0$	$0.15^{+0.05}_{-0.02}$	0.07	0.086[d] 0.280[d]					25 ± 5	7.42
$^{3}2$	$^{2}0$	<281	0.02						3 ± 2	0.15×10^{-3}
$^{3}2$	$^{1}2$	$\leq 3.4^{+2}_{-1.4}$	0.39			0.43		0.04	38 ± 10	98.29
$^{3}2$	$^{1}0$	$0.75^{+0.4}_{-0.2}$	0.01						59 ± 10	0.03
$^{4}2$	$^{2}2$		0.02			0.09		0.01	<1	5.47
$^{4}2$	$^{1}4$		1.68						2 ± 1	0.18
$^{4}2$	$^{1}2$	<0.8	0.04		$<1.2\times10^{-3}$[b]	0.29		−0.02	97 ± 2	91.98
$^{4}2$	$^{1}0$		0.12						1 ± 0.5	0.62
$^{2}4$	$^{2}2$	18 ± 9[b]	0.93						5 ± 2	0.01
$^{2}4$	$^{1}2$		1.66						95 ± 2	1.43
$^{3}4$	$^{3}2$		1.04						25 ± 5	0.03
$^{3}4$	$^{1}4$		6.75			0.03		−0.52	15 ± 5	83.29
$^{3}4$	$^{1}2$		0.16						52 ± 8	4.71
($^{1}6$)	$^{1}4$	17 ± 2.3[f]	15.08	4.12[g] 20.59[g] 15.06[h] 16.69[i]					100	100
$^{4}4$	$^{4}2$	40[b]	0.41						50 ± 5	0.03
$^{4}4$	$^{1}4$	<3[b]	0.70		$<1.5\times10^{-3}$[b]	0.02	$>\|0.5\|$[b]	−0.28	50 ± 5	45.00
$^{4}4$	$^{1}2$		0.01						2	0.34

[a] Reference 8.
[b] Reference 20.
[c] Reference 18.
[d] Reference 15. The first value corresponds to the $(f_{7/2})^n$ shell model; the second, to the $(f_{7/2})^n + (f_{7/2})^{n-1}(p_{3/2},f_{5/2})^1$ shell model.
[e] Reference 16.

TABLE III. (*Continued*)

[f] J. J. Simpson, W. R. Dixon, and R. S. Storey, Phys. Rev. 31, 946 (1973).
[g] Reference 14.
[h] Reference 11.
[i] Reference 17.
[j] Reference 20.

quasirotational structure in coexistence with a quasivibrational one, a fact which is generally established by the cluster-phonon model.[1] The main discrepancies appear in the calculated $B(E2;\ ^2 2 \rightarrow {}^2 0)$, $B(E2;\ ^2 4 \rightarrow {}^2 2)$ and $B(E2;\ ^4 4 \rightarrow {}^4 2)$ values which cannot be remedied with any of the possible set of parameters used.

The lifetimes are in general predicted within the order of magnitude of the experimental values.[19] A good agreement was achieved for the branching ratios.[19] The scarcity of experimental data on $B(M1)$ strengths[19] and mixing ratios[19,20] do not permit a meaningful comparison with experiment.

B. The ^{46}Ti nucleus

In Fig. 2 the experimentally observed positive-parity level sequence of ^{46}Ti [Fig. 2(A)] is compared with the results of our calculation [Fig. 2(B)]. There also are shown the values obtained by McCullen, Bayman, and Zamick (MBZ)[21] with the shell model using two different kinds of nucleon-nucleon interaction [Figs. 2(C) and 2(D)]. The results obtained by Rebel and Habs[22] with the generalized collective model of Greiner and Gneuss[23] are depicted in Fig. 2(E). It is important to point out that these calculations were performed by fitting the theoretical level schemes to the experimental positions of the low-lying levels, the $B(E2;\ ^1 2 \rightarrow {}^1 0)$ values, and adjusting the signs of the quadrupole moments to the experimental value. The MBZ calculations, although describing fairly well the observed levels, cannot account for the ^{2}0+ state which is reproduced by our calculations and those of Rebel and Habs.

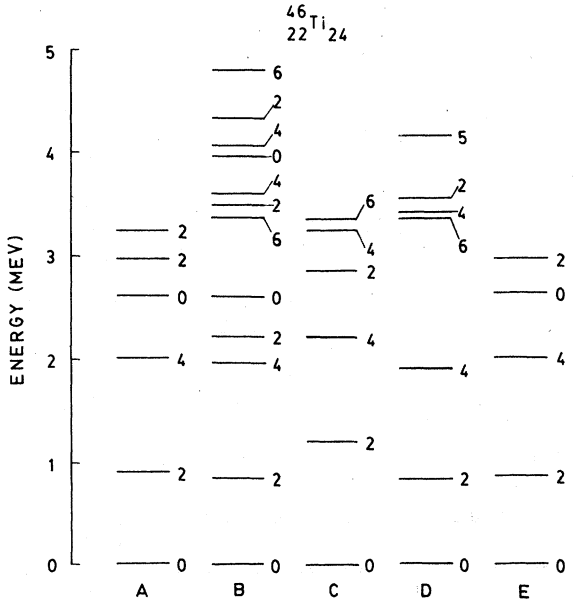

FIG. 2. Experimental and theoretical low-lying positive-parity level sequence for ^{46}Ti. A: Experiment (Ref. 8). B: Present model. C and D: Ref. 21. E : Ref. 22.

In Table IV the values of the electromagnetic properties experimentally observed are compared with the predictions of the present model. Concerning the static electric quadrupole moment of the ^{1}2+ state and $B(E2)$ strengths, they are also compared with those obtained with other models.[15,18,22] The experimental $Q(^1 2+)$ (Ref. 24) is reproduced by our calculations which also predict a large negative value for the ^{1}4+ state, similar to that already found in ^{44}Ti. The enhanced $E2$ transition probabilities from the ^{1}2, ^{1}4, and ^{1}6 states to the ground state and the hindered $B(E2;\ ^2 2 \rightarrow {}^1 0)$ strength reflects a parallelism with the ^{44}Ti nucleide. The agreement with experiment is satisfactory.

The available branching ratios[8] are in general reproduced by our calculations, and the lifetimes of the ^{1}2+ state is consistent with the two available experimental data.[8,25]

C. The ^{48}Ti nucleus

In Fig. 3 the experimental positive-parity level sequence of ^{48}Ti [Fig. 3(a)] is shown together with the predictions of the present model [Fig. 3(B)] and with those obtained with other models[21,22,26] [Figs. 3(C)-3(F)], respectively. It is to be noted that our calculated energy levels follow closely the trend of experimental data; indeed, the best fit is yielded by the present model.

Table V tabulates the experimental and calcu-

TABLE IV. Experimental and theoretical energy values of some low-lying positive-parity states for ^{46}Ti and those corresponding to the electromagnetic properties. The values calculated with others models are indicated by OM; the set of values for the effective proton and vibrator charges, and gyromagnetic ratios are indicated in the text.

	E (keV)		Q (eb)			$\mu(\mu_N)$	τ(ps)	
				Theory		Theory		Theory
$^{\kappa}I$	Exp.[a]	Theory	Exp.	I	OM	1	Exp.	$I+1$
$^{1}2$	889.4	865.7	-0.19 ± 0.10[b]	-0.215	-0.164[e]	0.579	10[a]	6.80
			-0.21 ± 0.06[c]		0.134[f]		4.69[h]	
			-0.28 ± 0.14[d]		-0.027[f]			
					-0.265[g]			
$^{1}4$	2009.9	1934.2		-0.214		1.810		1.65
$^{2}0$	2611	2602.9						
$^{2}2$	2962	2234.3		0.194		0.528		0.58
($^{3}2$)	3236	2511.3		0.189		3.785		4.7×10^{-3}

		$B(E2)$ (W.u.)			$B(M1)$ (W.u.)	δ	b (%)	
			Theory		Theory	Theory		Theory
$^{\kappa}I_i$	$^{\kappa}I_f$	Exp.	I	OM	1	$I+1$	Exp.[a]	$I+1$
$^{1}2$	$^{1}0$	18.30 ± 0.60[c]	25.19	12.66[e]			100	100
		19.80 ± 1.40[b]		9.70[f]				
				13.70[f]				
				19.68[g]				
				14.09[k]				
$^{1}4$	$^{1}2$	18.07 ± 2.04[j]	36.27	19.50[k]			100	100
$^{2}0$	$^{1}2$		6.21				100	79.55
$^{2}2$	$^{1}0$	0.21 ± 0.04[i]	0.45	0.008[f]			4	17.62
				0.13[f]				
				0.28[g]				
$^{2}2$	$^{1}2$	18.60 ± 4.20[i]	21.55	5.51[f]	0.002	2.65	96	82.38
				4.49[f]				
				11.91[g]				
($^{3}2$)	$^{1}0$						16	0.003
($^{3}2$)	$^{1}2$		0.09		0.35	0.02	84	97.52
($^{1}6$)	$^{1}4$	15.32 ± 8.17[j]	28.54	20.22[k]			100	100

[a] Reference 8.
[b] O. Häusser, D. Pelte, T. K. Alexander, and H. C. Evans, Nucl. Phys. A150, 417 (1970).
[c] Reference 24.
[d] N. V. de Castro Faría, J. Charbonneau, J. L. Ecuyer, and R. J. A. Levesque, Nucl. Phys. A174, 37 (1971).
[e] Reference 18.
[f] Reference 15. The first value corresponds to the $(f_{7/2})^n$ shell model; the second, to the $(f_{7/2})^n + (f_{7/2})^{n-1}(p_{3/2},f_{5/2})^1$ shell model.
[g] Reference 22.
[h] Reference 25.
[i] P. A. Assimakopoulos, T. Becker, C. Moazed, and D. M. van Patter, Bull. Am. Phys. Soc. 16, 60 (1971).
[j] W. Dehnhardt, O. C. Kistner, W. Kutschera, and H. J. Sann, Phys. Rev. C 7, 1471 (1973).
[k] Reference 17.

lated electromagnetic properties. The experimental $Q(^{1}2+)$ value is correctly achieved. However, the $E2$ transitions from the $^{1}2$, $^{1}4$, and $^{1}6$ levels to the ground states are systematically predicted at larger values than the experimental ones. It is natural to think that this difficulty would be overcome with the use of other values for the effective proton and vibrator charges. However, due to the fact that the gross trend in these values is reflected by our calculations no attempt to the best fit was pursued.

The lifetimes[8] and the branching ratios[18] are in general reasonably accounted for.

D. The ^{52}Ti nucleus

The experimentally observed positive-parity level sequence of ^{52}Ti is shown in Fig. 4(A) (Refs. 27, 28) and compared with the results of our calculations [Fig. 4(B)] and with those of shell-model calculations[29] [Fig. 4(C)]. In Table VI the experimental and calculated values of the

electromagnetic properties are tabulated. In the special case of ^{52}Ti the experiment does not provide either unambiguous spin or definite parity assignments for three levels out of the five reported ones. Since this fact does not permit a definite and quantitative comparison with experiment, it only should be made from a qualitative point of view.

The $^{1}2$, $^{1}4$, and $^{1}6$ states are well accounted for both in the present model and the shell model. The predicted $^{2}2+$ state at 2.36-MeV energy would correspond either with the experimentally found 2+ state at 2.26 MeV or with that at 2.43 MeV. The calculated $B(E2)$ strength and the lifetime for the $^{2}2$ state compare favorably with the experimental value corresponding to the $^{3}2$ state. However, since the $B(M1)$ strength and the value of the mixing ratio do not agree with experiment, the correspondence between them is not conclusive.

The rather large and negative values for the static quadrupole moments of the $^{1}2$, $^{1}4$, and $^{1}6$ states as well as the enhanced $E2$ strengths between them, and between the $^{1}2$ and the ground state present a strong resemblance to the features pointed out in the analysis of other titanium isotopes. The calculated lifetime for the $^{1}2$ state agree with experiment as well as do the calculated branching ratios for all the levels under consideration. However, the precise knowledge of their spin and parities does not permit one to arrive at a definite conclusion.

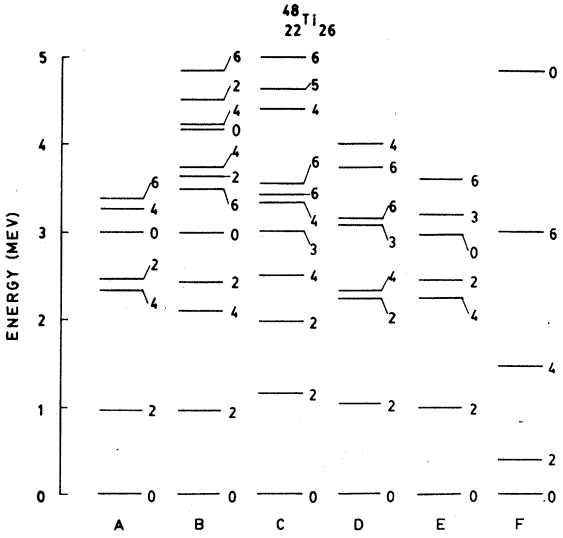

FIG. 3. Experimental and theoretical low-lying positive-parity level sequence for ^{48}Ti. A: Experiment (Ref. 8). B: Present model. C and D: Ref. 21. E: Ref. 22. F: Ref. 26.

IV. GENERAL CONCLUSIONS

With the cluster-phonon model used in the present work we were able to reproduce not only the general trend of the experimental data corresponding to the doubly even titanium isotopes but also to describe their decay properties, some of them not hitherto predicted by any model. It is worthwhile to note that our calculations involve only three adjustable parameters, namely, the pairing interaction strength G, the quadrupole deformation β and the phonon energy $\hbar\omega$ (see Table I), which were smoothly varied, from one nucleide to another, within reasonable limits. It should also be emphasized that no attempt to best fit individual properties was pursued since our scope was delimited by the "physics" of the problem under investigation rather than by the search for the "best set" of the parameters involved.

It seems important to recall that our calculations predict (and reflect the experimental situation when data are available) rather large negative quadrupole moments for some low-lying states

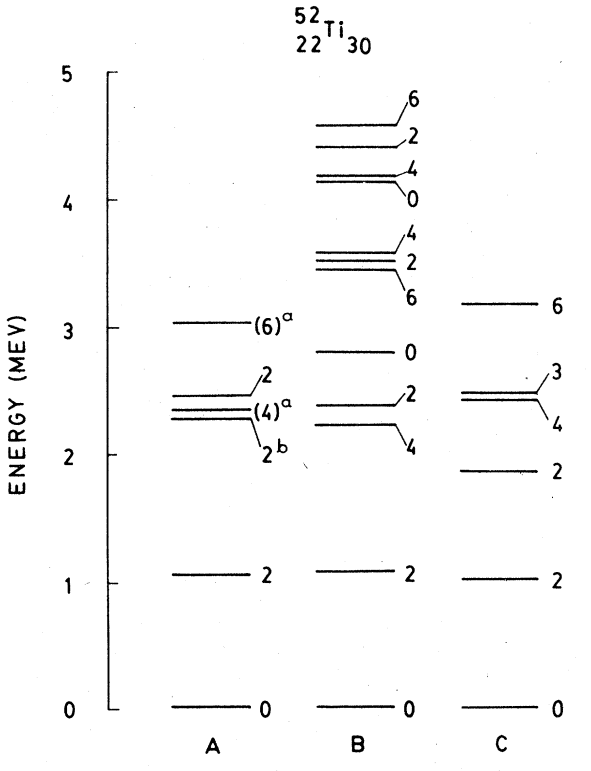

FIG. 4. Experimental and theoretical low-lying positive-parity level sequence for ^{52}Ti. A: Experiment (Ref. 27); the levels indicated with a are taken from Ref. 28, and those with b have not been assigned parity. B: Present model. C: Ref. 29.

TABLE V. Experimental and theoretical energy values of some low-lying positive-parity states for ^{48}Ti and those corresponding to the electromagnetic properties. The values calculated with others models are indicated by OM; the set of values for the effective proton and vibrator charges, and gyromagnetic ratios are indicated in the text.

	E (keV)		Q (eb)			$\mu(\mu_N)$	τ(ps)	
				Theory		Theory		Theory
$^{\kappa}I$	Exp.[a]	Theory	Exp.	I	OM	1	Exp.[a]	$I+1$
$^{1}2$	983.4	971.7	-0.22 ± 0.08[b] -0.13 ± 0.08[c]	−0.204	−0.092[d] −0.173[e] 0.018[c] −0.136[c]	0.590	4.3 6.4[c]	3.90
$^{1}4$	2295.5	2106.7		−0.217		1.968	1.7	1.18
$^{2}2$	2420.3	2392.5		0.182		0.570	0.044 ± 0.012[f]	0.44
$^{2}0$	2997.4	2993.8					0.11	0.16
($^{2}4$)	3239.7	3748.9		−0.185		4.850	0.03	0.007
($^{1}6$)	3333	3473.7		−0.311		6.800	12.80 ± 1.2[g]	0.64

		$B(E2)$ (W.u.)			$B(M1)$ (W.u.)		δ		b (%)	
			Theory		Theory			Theory		Theory
$^{\kappa}I_i$	$^{\kappa}I_f$	Exp.	I	OM	1	Exp.[c]		$I+1$	Exp.[c]	$I+1$
$^{1}2$	$^{1}0$	13.30 ± 1.10[b]	23.31	7.72[c] 10.25[c] 9.07[d] 13.24[e] 10.52[i]					100	100
$^{1}4$	$^{1}2$	9.16 ± 2.10[i]	35.40	14.76[i]					100	100
$^{2}2$	$^{1}0$	$2.40^{+\infty}_{-1.90}$[h]	0.30	0.13[c] 1.48[c] 0.16[e]					4	13.35
$^{2}2$	$^{1}2$	$17.50^{+\infty}_{-15}$[h]	23.26	12.74[c] 27.16[c] 12.74[e]	0.003	$\lvert 0.15 \rvert$		2.59	96	86.64
$^{2}0$	$^{1}2$		13.44						100	95
($^{1}6$)	$^{1}4$	5.11 ± 0.48[i]	25.70	15.05[i]					100	100

[a] Reference 8.
[b] O. Häusser, D. Pelte, T. K. Alexander, and H. C. Evans, Nucl. Phys. A150, 417 (1970).
[c] Reference 15. The first value corresponds to the $(f_{7/2})^n$ shell model; the second, to the $(f_{7/2})^n + (f_{7/2})^{n-1}(p_{3/2},f_{5/2})^1$ shell model.
[d] Reference 18.
[e] Reference 22.
[f] V. K. Rasmussen, Phys. Rev. C 13, 631 (1976).
[g] B. A. Brown, D. B. Fossan, J. M. McDonald, and K. A. Snover, Phys. Rev. C 9, 1033 (1974).
[h] C. D. Kavaloski and W. J. Kossler, Phys. Rev. 180, 971 (1969).
[i] Reference 17.

as well as enhanced $E2$ transition between them. On the other hand, inspection of Table II shows that the $^{1}0$, $^{1}2$, $^{1}4$, $^{2}0$, and $^{2}2$ levels are mainly built on the $(f_{7/2})^2 0$ pair coupled to zero-, one-, and two-phonon states. A point which deserves special attention is that the $^{1}6$ state is based mainly on the $(f_{7/2})^2 6$ pair, a situation already found in the case of ^{56}Fe studied by Paar[2] with the same model as used here. Since it seems of importance to compare the present results with those of ^{56}Fe, we repeated the calculations performed by Paar using our own computational program in order to have available some additional information. From the comparison between the strongest $E2$ transitions corresponding to ^{56}Fe and the titanium isotopes emerges the existence of a second quasirotational band. In the present case the new band lies above the ground state band which is the inverse situation to that found in ^{56}Fe. This set of features—when considered together—

TABLE VI. Experimental and theoretical energy values of some low-lying positive-parity states for ^{52}Ti and those corresponding to the electromagnetic properties. The values calculated with other models are indicated by OM; the set of values for the effective proton and vibrator charges, and gyromagnetic ratios are indicated in the text.

	E (keV)		Q (eb) Theory		$\mu(\mu_N)$ Theory		τ (ps)	Theory
$^{\kappa}I$	Exp.[a]	Theory	I	OM	1	OM	Exp.[c]	$I+1$
$^{1}2$	1049.8 ± 0.6	1064.6	−0.154	−0.12[b]	0.461	0.82[b]	$4.80^{+8.0}_{-2.1}$	3.06
$^{2}2(\pm)$	2264.5 ± 1.0	2365.8	0.134		0.452		$0.05^{+0.03}_{-0.02}$	0.73
$(^{1}4)$	2317[d]	2195.0	−0.173		1.633			1.40
$^{3}2$	2431.7 ± 1.2	3540.1	0.188		3.574		≤0.10	7.32
$(^{1}6)$	3027[d]	3464.6	−0.295		7.236		36.7 ± 6.3	1.25

		$B(E2)$ (W.u.)		$B(M1)$ (W.u.)		δ		b (%)	
			Theory		Theory		Theory		Theory
$^{\kappa}I_i$	$^{\kappa}I_f$	Exp.[c]	I	Exp.[c]	1	Exp.[c]	$I+1$	Exp.[c]	$I+1$
$^{1}2$	$^{1}0$	12.0^{+9}_{-7}	16.90					100	100
$^{2}2(\pm)$	$^{1}0$		0.07					5	5.80
$^{2}2(\pm)$	$^{1}2$		21.07	0.37	0.002	−0.03 ± 0.10	2.54	95	94.19
$^{3}2$	$^{1}0$		0.05					15	0.29
$^{3}2$	$^{1}2$	≥11	0.03	≥0.12	0.290	0.39 ± 0.08	0.02	85	98.11
$(^{1}6)$	$(^{1}4)$	10.6 ± 1.8	17.13						100

[a] Reference 27.
[b] Reference 29.
[c] J. G. Pronko, T. T. Bardin, J. A. Becker, T. R. Fisher, R. E. McDonald, and A. R. Poletti, Phys. Rev. C 9, 1430 (1974).
[d] Reference 28.

favors the assumption of a quasirotational structure in coexistence with a quasivibrational one, a fact which is generally established by the classical semimicroscopic model.

This work was partially supported by the Consejo Nacional de Investigaciones Cientificas y Técnicas, Argentina.

[1] G. Alaga, in *Cargese Lectures in Physics*, edited by M. Jean (Gordon and Breach, New York, 1969), Vol. 3, p. 579.
[2] V. Paar, Nucl. Phys. A185, 544 (1972).
[3] S. M. Abecasis, C. A. Heras, and F. Krmpotic, Phys. Rev. C 11, 1015 (1975).
[4] W. J. Gerace and A. M. Green, Nucl. Phys. A113, 641 (1968).
[5] A. Bohr and B. R. Mottelson, *Nuclear Physics* (Benjamin, New York, 1969), Vol. I.
[6] P. H. Stelson and L. Grodzinz, Nucl. Data A1, 2 (1965).
[7] L. S. Kisslinger and R. A. Sorensen, Rev. Mod. Phys. 35, 853 (1963).
[8] E. Browne (private communication).
[9] S. B. Khadkikar and B. Banerjee, Nucl. Phys. A129, 220 (1969).
[10] M. Danos and V. Gillet, Phys. Rev. 161, 1034 (1967).
[11] K. H. Bhatt and J. B. McGrory, Phys. Rev. C 3, 2293 (1971).
[12] D. H. Kong-A-Siou, J. F. Braundet, J. P. Longequeue, N. Longequeue, and B. Vignon, Nucl. Phys. A197, 568 (1972).
[13] P. W. M. Glaudemans, P. J. Brussaard, and B. H. Wildenthal, Nucl. Phys. A102, 593 (1967).
[14] J. J. Kolata, J. W. Olness, and E. K. Warburton, Phys. Rev. C 10, 1663 (1974).
[15] P. M. S. Lesser, D. Cline, P. Goode, and R. N. Horoshko, Nucl. Phys. A190, 597 (1972).
[16] W. R. Dixon, R. S. Storey, and J. J. Simpson, Nucl. Phys. A202, 579 (1973).
[17] A. K. Dhar and K. H. Bhatt, Phys. Rev. C 16, 792 (1977).
[18] S. K. Sharma, International Centre for Theoretical Physics, Report No. IC/74/62, 1974 (unpublished).
[19] W. R. Dixon and R. S. Storey, Phys. Rev. C 15, 1896 (1977).
[20] J. J. Simpson, W. R. Dixon, and R. S. Storey, Phys. Rev. C 4, 443 (1971).
[21] J. D. McCullen, B. F. Bayman, and L. Zamick, Phys. Rev. 134, B515 (1964).
[22] H. Rebel and D. Habs, Phys. Rev. C 8, 1391 (1973).
[23] G. Gneuss and W. Greiner, Nucl. Phys. A171, 449 (1971).
[24] C. W. Towsley, D. Cline, and R. N. Horoshko, Nucl. Phys. A250, 381 (1975).
[25] V. S. Shirley and C. M. Lederer, Lawrence Berkeley Laboratory, Report No. LBL-3450, 1974 (unpublished).
[26] K. Allaart, K. Goeke, H. Müther, and A. Faessler, Phys. Rev. C 9, 988 (1974).
[27] J. G. Pronko, T. T. Bardin, J. A. Becker, T. R. Fisher, R. E. McDonald, and R. A. Poletti, Phys. Rev. C 10, 1249 (1974).
[28] B. A. Brown, D. B. Fossan, A. R. Poletti, and E. K. Warburton, Phys. Rev. C 14, 1016 (1976).
[29] H. Horie and K. Ogawa, Nucl. Phys. A216, 407 (1973).